

2014

Nano-Scale Spinning Detonation in a Condensed Phase Energetic Material

Vasily V. Zhakhovsky
University of South Florida

Mikalai Budzevich
University of South Florida, mbudzevi@mail.usf.edu

Aaron C. Landerville
University of South Florida, alanderv@gmail.com

Ivan I. Oleynik
University of South Florida, oleynik@usf.edu

Carter T. White
Naval Research Laboratory, Washington DC

Follow this and additional works at: http://scholarcommons.usf.edu/phy_facpub

Scholar Commons Citation

Zhakhovsky, Vasily V.; Budzevich, Mikalai; Landerville, Aaron C.; Oleynik, Ivan I.; and White, Carter T., "Nano-Scale Spinning Detonation in a Condensed Phase Energetic Material" (2014). *Physics Faculty Publications*. Paper 9.
http://scholarcommons.usf.edu/phy_facpub/9

This Article is brought to you for free and open access by the Physics at Scholar Commons. It has been accepted for inclusion in Physics Faculty Publications by an authorized administrator of Scholar Commons. For more information, please contact scholarcommons@usf.edu.

Nano-scale spinning detonation in a condensed phase energetic material

Vasily V Zhakhovsky¹, Mikalai M Budzevich¹,
Aaron C Landerville¹, Ivan I Oleynik¹ and Carter T White²

¹University of South Florida, 4202 East Fowler Avenue, Tampa, Florida 33620-5700, USA

²Naval Research Laboratory, Washington DC 20375-5320, USA

E-mail: 6asi1z@gmail.com

Abstract. A single-headed spinning detonation wave is observed in molecular dynamics simulations of a condensed phase detonation of an energetic material confined to a round tube. The EM is modeled using a modified AB reactive empirical bond order (REBO) potential. The simulated spinning detonation is similar to those observed in the gas phase. However, in addition to the incident, oblique, and transverse shock waves well known from gas-phase spinning detonations, a contact shock wave generated by a contact discontinuity is uncovered in our MD simulations.

1. Introduction

Gas-phase detonations close to failure are known to spontaneously develop complex two and three dimensional structures such as cellular and pulsating patterns that prevent their collapse. Contained in these structures are extreme regions where the exothermic chemical reactions driving the detonation are greatly enhanced. Although well known in the gas phase [1, 2], such complex structures have not yet been observed in the condensed phase with the exception of dilute liquids [3–5]. This is not surprising, as processes in condensed phase detonations occur at much smaller length and time scales making the experimental observation of such detonation microstructure extremely difficult. On the other hand, these short time and length scales are ideal for molecular dynamics (MD) simulations. Indeed, Helm *et. al* [6] recently found that a variant [7] of perhaps the simplest model of a condensed-phase explosive, the well-known AB model [8–10], could support a cellular detonation in MD simulations of 2D samples. More recently, we have shown that a modified 3D version of the AB model can support detonation structures ranging from laminar, to cellular, to turbulent depending on the boundary conditions and the reaction barrier E_b for the half reactions $A + AB \rightarrow A_2 + B + 3\text{eV}$ and $B + BA \rightarrow B_2 + A + 3\text{eV}$ that support the detonation [11]. Although at a much smaller scale, these structures closely parallel those observed in the gas phase. Hence, such simulations provide a new probe into the nature of these patterns and how they can arise.

Also observed in our earlier MD simulations was a so called transverse detonation [11]. Such a detonation, however, cannot be ultimately stable under experimental conditions because the transverse wave will eventually collide with the sample walls causing the transverse detonation to transform into a cellular one. Thus, the transverse detonation is a result of the periodic boundary conditions assumed in the simulations. Potentially this problem can be avoided by



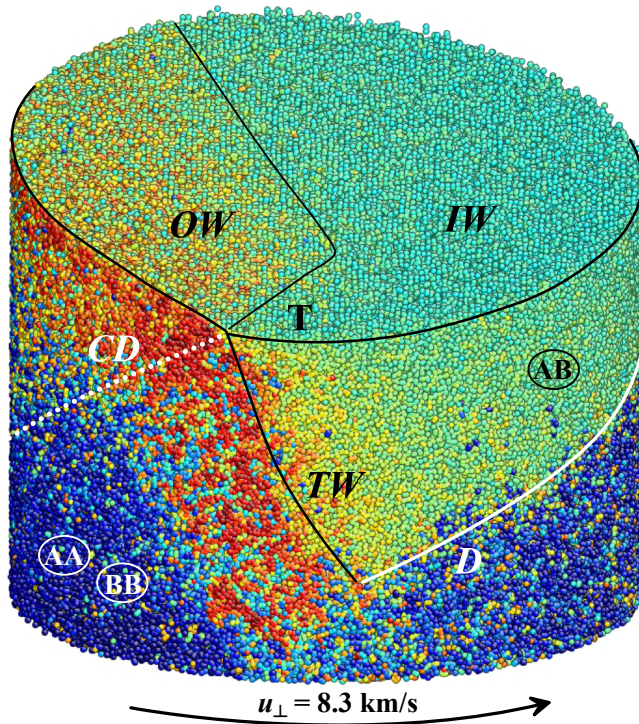


Figure 1. Snapshot of the single-headed spinning detonation propagating in the vertical direction with velocity $u_{\parallel} = 8.37$ km/s in an AB solid with $E_b = 0.367$ eV confined to a tube with radius $R_0 = 15.6$ nm. Only atoms in the compressed material are shown. Aquamarine colored atoms are in the unreacted AB material experiencing a relatively low pressure. Red-colored atoms are those in the highly-pressurized AB material. The product molecules AA and BB are colored dark blue. Black solid lines correspond to the three shock waves IW, OW, and TW described in the text. Flows behind OW and TW are separated by a contact discontinuity CD (dashed white line). A contact discontinuity D between reactants compressed by IW and hot products behind OW is shown by a white solid line.

initiating the detonation in a tube which could result in a spinning detonation. Indeed, we show herein that this is the case. In fact, spinning detonations in round tubes have long been known in the gas phase, where Campbell and Woodhead decades ago reported a localized region near a tube wall where intense chemical reactions occur [12]. This localized region known as a detonation head follows a helical path as the detonation propagates along the tube. Later it was found that the spinning head is due to extra compression by both transverse and oblique shock waves acting in concert with a relatively weak incident shock wave, all three intersecting in a Mach configuration [13,14]. As we shall see, the condensed phase spinning detonation observed in our AB simulations in a tube behaves in a similar fashion but also exhibits a fourth shock wave generated by a contact discontinuity. This fourth shock wave has not been observed before in spinning detonations.

2. Simulation technique

The spinning detonation was simulated by moving window-molecular-dynamics (MW-MD) [15–18]. A solid AB sample was confined to a the tube of radius $R_0 = 15.6$ nm by using a steep quadratic potential $U_w = a(\rho_i - R_0)^2$ applied to all atoms i with radial distance ρ_i from the axis of the tube such that $\rho_i > R_0$. The particular version of the AB model used in these simulations is described in detail elsewhere [19]. Throughout, the reaction barrier E_b is taken as 0.367 eV, which brings the detonation close to failure. The simulation was started by using the flow pattern from a detonating 3D sample tailored to fit within the tube by removing all atoms with $\rho_i > R_0$.

Although results reported below are restricted to a 15.6 nm radius sample with a reaction barrier of 0.367 eV, we have found that the morphology of the spinning detonation structure depends on E_b and R_0 . For example, for $E_b = 0.245$ eV, the detonation structure changes from a single to a multi-headed detonation for samples with radii above 15 nm, while for $E_b = 0.367$ eV a multi-headed detonation develops at much larger tube radii above ~ 30 nm.

3. Atomic and flow structure of a single-headed spinning detonation

For $E_b = 0.367$ eV, the MW-MD simulation shows that an initially planar detonation front propagating in a tube of radius $R_0 = 15.6$ nm becomes unstable by developing multiple longitudinal density fluctuations. After several tens of picoseconds a steady, single-headed, spinning detonation is established. Figures 1 and 2 show atomic and flow structures, respectively, of this spinning detonation. The atoms with very high potential energy within the TW front are colored red in figure 1, while atoms colored dark blue have the atomic potential energy of atoms in AA and BB product molecules following the reaction. The flow maps of potential energy per atom and temperature shown in figure 2 were obtained by averaging the atomic values of these quantities over a shell of $\rho \in [11, 15]$ nm on a regular cylindrical mesh with $180 \text{ cells} \times 378 \text{ cells}$ in the corresponding range of azimuth $\phi \in [-\pi, \pi]$ and tube length of 197 nm. Atoms with $\rho_i > 15$ nm were not included in these averages because they are too close to the repulsive tube wall potential at 15.6 nm. The pixels in figure 2 correspond to approximately 50 to 150 atoms, depending on the local density.

From figure 1 it is easy to identify the three shock fronts, also seen in gas-phase detonations. They are the weak incident shock wave IW; the transverse shock wave TW; and, the oblique shock wave OW. The intersection point of the shock fronts T lying on the tube surface rotates counterclockwise with a circumferential velocity $u_{\perp} = 8.3$ km/s, while propagating in the positive axial direction with velocity $u_{\parallel} = 8.37$ km/s. In the coordinate system where the detonation head is stationary, the AB molecules in the uncompressed solid enter the leading IW and OW fronts with velocity 11.8 km/s at an angle of $\varphi = 45.2^\circ$ with the tube axis, as shown in figure 3. Therefore, the incoming flow of AB molecules has a large inclination angle with respect to the IW front, which causes the cold AB molecules passing through the IW front to be noticeably deflected, thus gaining a clockwise angular velocity (*i.e.* toward to the TW front) in the MW-MD coordinate system.

The three shock waves IW, TW, and OW, produce three distinct zones behind the spinning AB detonation front clearly visible in figure 2. Two of these zones are termed stripes as they extend all the way around the surface of the tube, as can be seen from figure 2. Zone 1, which does not extend completely around the tube, is generated by IW. This incident shock wave is relatively weak and does not induce reactions in the compressed AB solid as is seen from the potential energy of atoms colored by aquamarine in figure 1, which corresponds to the potential energy of an atom in a AB molecule. However, the AB material, pre-compressed and pre-heated

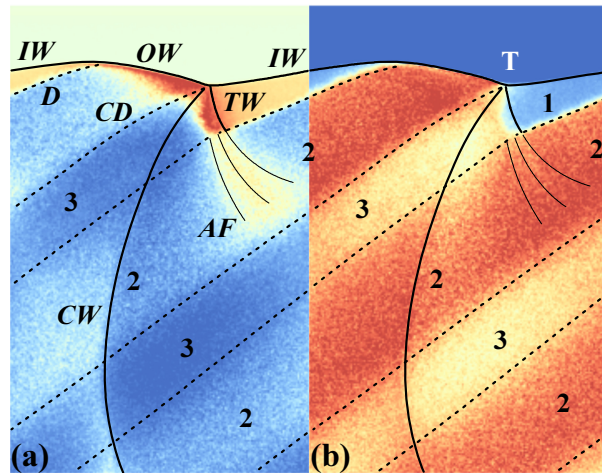


Figure 2. Flow maps of (a) potential energy and (b) temperature in a spinning detonation propagating in AB solid confined to a tube. The vertical is aligned with the tube axis, and the circumferential distance on the tube wall is along the horizontal axis. The solid lines show four shock-wave fronts in the neighborhood of the point T, including the weak IW, the strong TW and OW, and the contact shock wave CW generated by CD. Three zones in the material at different states are formed by the detonation front. IW produces the compressed but relatively cold reactants in zone 1, which later are ignited by TW leading to the formation of stripe 3 consisting of relatively cold products at low pressure. Reactions after OW produce relatively hot products at high pressure in stripe 2, which generates CW.

by IW to relatively low pressures of 27–28 GPa and temperatures 1.6–1.8 kK, flows in zone 1 toward the strong TW shock in a coordinate system where the detonation is stationary, as illustrated by figures 2 and 3. In such a non-inertial reference frame the wave configuration is at rest while the material flows through the static shock fronts and reaction zones. The TW produces high compression 90–98 GPa and heating to 6–6.5 kK of the AB material, which rapidly ignites the reactants which are then converted to products within a narrow reaction zone behind TW. Over this thin reaction zone the very high pressure in TW drops to 14–16 GPa causing acceleration of the mass flow to 11.4 km/sec in the reference frame where the detonation head is stationary. Thus, stripe 3 made up of a fast low-pressure flow consisting of relatively cold products with temperatures in the range 4.7–5 kK is formed. In contrast, stripe 2 produced by the reaction zone after OW is a hot flow with slightly lower mass velocity 9.1 km/sec in the same reference frame. It consists of products with a notably higher pressures 27–30 GPa and temperatures 8.7–9 kK than in stripe 3.

Note that TW front cannot be extended beyond zone 1 containing reactants to the hot product flow in stripe 2 as a shock front, because there can be no reaction zone behind a shock wave propagating in the products. Instead, TW decays into a fan of acoustic compression waves AF with the pressure in AF decreasing with distance from the end of the TW front, as depicted in figure 2. In general, all shock fronts existing in a steadily propagating self-sustained detonation must have some kind of support or they will decay with time. In addition, note that the strength and slope of OW decreases away from T to the point that it abruptly transforms into IW where reactions cease.

From figures 1 and 2 it is also easy to identify two contact discontinuities in the spinning AB detonation: D separating the flow of reactants behind IW in zone 1 from the flow of products behind OW in stripe 2; and, CD separating the flow of products behind OW in stripe 2 from the flow of products behind TW in stripe 3. As described above, across CD there is a significant pressure difference generated just behind the OW and TW reaction zones. This causes the high pressure stripe 2, behaving as a piston, to generate an additional shock wave CW to equalize pressures after CW there. As a result the pressure in stripe 2 decreases to 19–20 GPa, and CD bends towards stripe 3. After nearly a complete revolution CW contacts CD. At this point the density in stripe 2 is below that of stripe 3 resulting in a transmitted shock wave still denoted by CW but moving at a higher speed. This results in appreciable bending of CW at the 2-3 interface seen in the downstream flow near the bottom of figure 2. Note that CW does not introduce additional stripes but rather alters the flow variables within stripes. Shock waves such as CW have not been observed in gas-phase detonation experiments and continuum simulations. Instead a detonation head with double Mach configuration was experimentally detected. For examples, see figure 11 in reference [20] and figure 7.24 in reference [1].

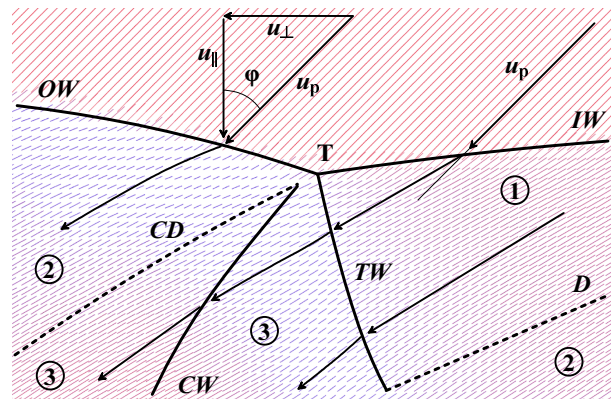


Figure 3. Mass velocity field and wave configuration in the vicinity of T in a spinning detonation propagating in AB solid confined to a tube. The point T spins counterclockwise in the tube with a circumferential velocity $u_{\perp} = 8.3$ km/s and an axial velocity $u_{\parallel} = 8.37$ km/s. Particle velocities are shown in the reference frame where the detonation head is stationary.

4. Concluding Remarks

The structure of the spinning detonation described above is remarkably similar to that observed in detonating gases [20–22] with two exceptions. In contrast to the gas phase, where three-wave Mach configurations are observed, an unexpected four-wave shock configuration in the neighborhood of T has been found in the spinning detonation in the AB solid. Also, the simulated spinning detonation pattern does not exhibit the double Mach configuration with additional discontinuities observed in gas phase detonation. This could be due to the fact that detonation in the condensed phase AB material develops at a very short length scale, on the order of tens interatomic distances, which might prevent complex fine structure from developing in such a confined spatial region.

Acknowledgments

The work at USF and NRL was supported by NRL and ONR, respectively. The work at USF was also supported by NSF, DTRA and an USF Research Faculty Pathway Grant. Simulations were performed using the NSF XSEDE facilities, the USF Research Computing Cluster, and the computational facilities of the Materials Simulation Laboratory at USF.

References

- [1] Fickett W and Davis W C 1979 *Detonation* (Berkeley: University of California)
- [2] Lee J H S 2008 *The Detonation Phenomenon* (Cambridge: Cambridge University Press)
- [3] Dremin A and Rosanov O 1961 *Dokl. Akad. Nauk SSSR* **139** 137–139
- [4] Mallory H D 1976 *J. Appl. Phys.* **47** 152–156
- [5] Matsukov D, Solovev V and Sorokin S 1994 *Combust. Explos. Shock Waves* **30**(4) 563
- [6] Heim A J, Grønbech-Jensen N, Kober E M and Germann T C 2008 *Phys. Rev. E* **78** 046710
- [7] Heim A J, Grønbech-Jensen N, Kober E M, Erpenbeck J J and Germann T C 2008 *Phys. Rev. E* **78**(4) 046709
- [8] Brenner D W, Robertson D H, Elert M L and White C T 1993 *Phys. Rev. Lett.* **70** 2174–2177; 1996 *ibid.* **76**, 2202
- [9] Rice B M, Mattson W, Grosh J and Trevino S F 1996 *Phys. Rev. E* **53**(1) 611–622
- [10] For a review, see White C T, Swanson D R, and Robertson D H 2001 in *Chemical Dynamics in Extreme Environments*, edited by Dressier R (London: World Scientific) Chap. 11, 547–592
- [11] Zhakhovsky V V, Budzevich M M, Landerville A C, Oleynik I I and White C T 2013 *J. Phys.: Conf. Ser.* Submitted for publication
- [12] Campbell C and Woodhead D W 1926 *J. Chem. Soc.* 3010–3021
- [13] Courant R and Friedrichs K O 1948 *Supersonic Flow and Shock Waves* (New York: Interscience Publishers)
- [14] Ben-Dor G 2007 *Shock Wave Reflection Phenomena* 2nd ed (Berlin: Springer)
- [15] Zhakhovskii V V, Nishihara K and Anisimov S I 1997 *JETP Lett.* **66** 99–105
- [16] Anisimov S I, Zhakhovskii V V and Fortov V E 1997 *JETP Lett.* **65** 755–761
- [17] Zhakhovsky V V, Budzevich M M, Oleynik I I and White C T 2011 *Phys. Rev. Lett.* **107** 135502
- [18] Budzevich M M, Zhakhovsky V V, White C T and Oleynik I I 2012 *Phys. Rev. Lett.* **109** 125505
- [19] Zhakhovsky V V, Budzevich M M, Landerville A C, Oleynik I I and White C T *submitted to Phys. Rev. E*
- [20] Schott G L 1965 *Phys. Fluids* **8** 850–865
- [21] Voitsekhovskii B, Mitrofanov V and Topchiyan M Y 1966 *The structure of a detonation front in gases.* (Wright Patterson AFB Rept. FTD-MT-64-527 (AD-633,821))
- [22] Tsuboi N, Eto K and Hayashi A 2007 *Combust. Flame* **149** 144 – 161